Transient complexes of haem proteins

Volkov, O.M.

Chapter VI

Increased affinity in the complex of yeast cytochrome c and cytochrome c peroxidase

Abstract

We report the study of T12A Cyt *c* – CcP complex using isothermal titration calorimetry (ITC), nuclear magnetic resonance (NMR) chemical shift perturbation mapping, and site-specific spin-labelling in combination with paramagnetic relaxation enhancement (PRE) NMR spectroscopy. Contrary to our expectations, the mutation enhances the binding by an order of magnitude, with the favourable enthalpy term responsible for the additional stabilization. Moreover, the thermodynamic parameters for the binding of T12A Cyt *c* are in a better agreement to the theoretically predicted values than those for the wild-type protein. At the same time, the solution structure of the dominant form of T12A Cyt *c* – CcP complex is the same as that of the wt complex (Chapter III), and – as evidenced by both chemical shift perturbation and PRE analyses – the mutation has very little influence on the protein dynamics within the complex. Thus, our results suggest that T12A mutation of Cyt *c* increases the binding affinity of Cyt *c* – CcP complex without affecting the specificity of the interaction. We argue that the affinity increase is mediated by ordering of water molecules at the interface, which would also explain the observed trends in the temperature-dependence of the thermodynamic binding parameters.

The results presented in this chapter will be published as:

Volkov, A. N., Worrall, J. A. R. & Ubbink, M. Mutation-induced increase of binding affinity in the complex of yeast cytochrome *c* and cytochrome *c* peroxidase (manuscript in preparation).

Introduction

Many biochemical processes are mediated by transient protein-protein interactions which purpose is to relay information – be it a chemical message in a signal transduction cascade or a reducing equivalent in an electron transfer chain – from one partner to the other (Chapter I). Given the variety of potential interaction partners in the cellular milieu, the efficiency, selectivity, and velocity of such relay are often bewildering. Being messengers between different biomolecules, the proteins that form transient complexes can interact with several partners. Such promiscuity of protein-protein association poses an interesting dilemma: on one hand, the specificity of the interaction should be low enough to allow a protein to recognize several structurally distinct partners but, on the other hand, the specificity should be sufficiently high so that the protein interacts exclusively with its partners, avoiding all other cellular components. In fact, these two factors are finely balanced, so that only a narrow margin of specificities towards different partners is maintained, enabling an effective functioning of the transient complexes.

Requirement of a high turn-over in the ET or signal transduction processes imposes another condition on the properties of transient protein complexes: as their name implies, they should be short-lived. As the lifetime of a complex is determined by its dissociation rate constant (k_{off}) that, in turn, affects the binding constant ($K_B = k_{on}/k_{off}$), the millisecond-scale lifetimes of transient complexes, *i.e.* $k_{off} \geq 10^3\ s^{-1}$, give rise to the binding affinities in the μM – mM range (Chapter I). In other words, transient protein complexes are weak.

There is no simple relationship between affinity and specificity of transient protein-protein interactions, yet the two are clearly connected. In general, stronger complexes are often more specific and vice versa. However, a drastic change in specificity of a protein complex could be accompanied by only a moderate change in affinity (Chapter V), suggesting that different factors determine the two properties. Unfortunately, the determinants of the affinity and specificity of transient protein interactions remain poorly understood[4]. To probe deeper into the source of binding affinity and specificity in protein-protein complexes, we have performed mutational analysis of two interfacial residues, R13

and T12 of Cyt *c*, in the transient ET complex between Cyt *c* and CcP. While the former is reported in the previous chapter, the latter is the subject of the present report.

Using two independent techniques, ITC and NMR spectroscopy, we have studied the binding of wt and T12A Cyt *c* to CcP at different temperatures. In addition, we have used PRE NMR spectroscopy to determine the solution structure of and ascertain the protein dynamics in T12A Cyt *c* – CcP complex. Our results suggest that T12A mutation of Cyt *c* increases the affinity of the complex without affecting the specificity of the interaction. We show that the affinity increase is likely mediated by ordering of water molecules at the interface.

Results and Discussion

NMR chemical shift perturbation analysis

To investigate the influence of T12A mutation of Cyt *c* on the binding to CcP, we have performed a comparative NMR analysis of the wt and the variant complexes. The NMR spectra of the free T12A Cyt *c* are similar to those of the wt protein (Figure 6.1). Large differences in chemical shifts are found only for the resonances of the residues located around the mutation site, T12, indicating that the mutation does not perturb the overall structure of the protein.

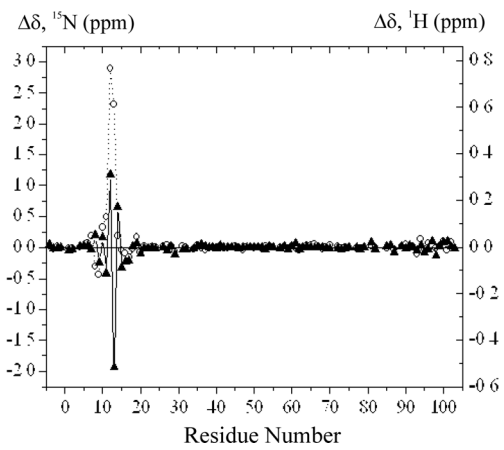

Figure 6.1. **Effects of T12A mutation on the chemical shifts of Cyt *c* backbone amide atoms.** Δδ is the difference between the chemical shifts in the 2D [^{15}N, ^{1}H] HSQC spectra of T12A and the wt ^{15}N Cyt *c* for backbone amide nitrogen (open circles) and proton (filled triangles) nuclei.

The binding-induced chemical shift perturbations of certain Cyt *c* resonances in the complex with CcP, can be monitored in the 1D and 2D NMR spectra (Figure 6.2). As the complex is in fast exchange on the NMR time-scale (Chapter V), a single set of resonances is observed. The size of the binding shifts – extrapolated to the 100 %

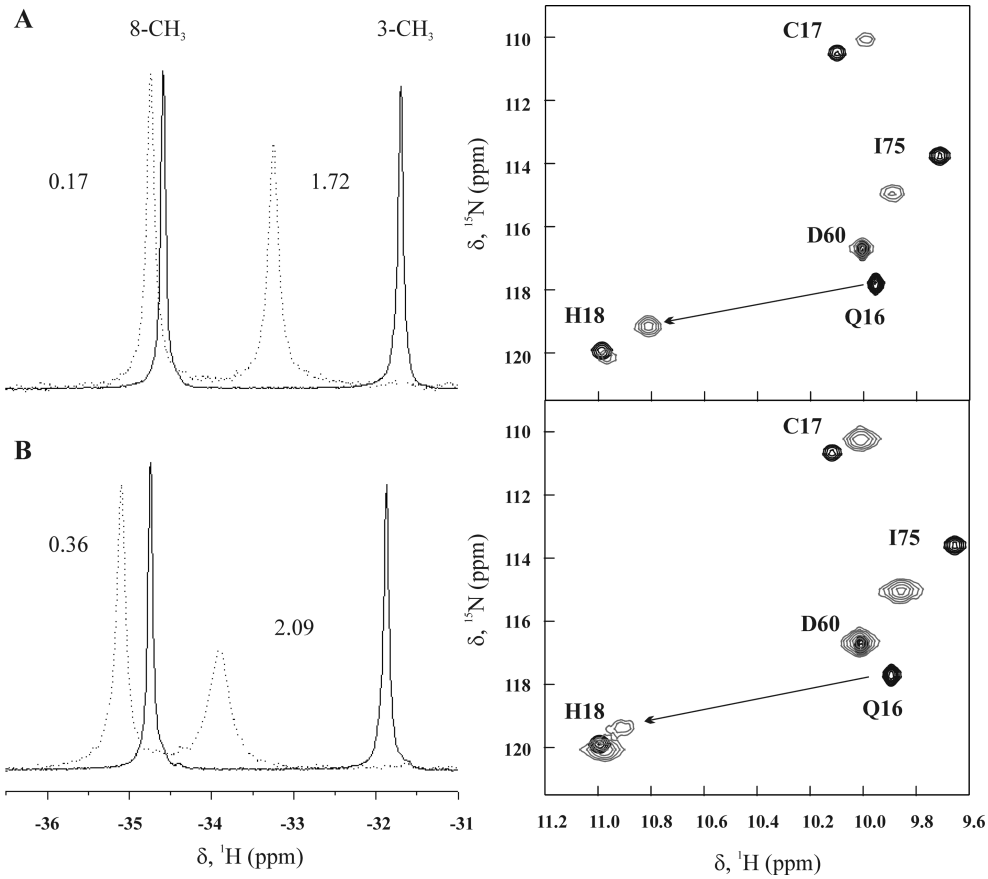

Figure 6.2. **Chemical shift perturbations of Cyt *c* resonances upon binding to CcP.** The binding shifts of wt (**A**) and T12A (**B**) Cyt *c* in the presence of 1 molar equivalent of CcP. (*left*) Downfield hyperfine-shifted resonances in the 1D ^{1}H NMR spectra of free (solid line) and bound (broken line) Cyt *c*. The assignments of the Cyt *c* peaks are indicated. The chemical shift perturbations, in ppm, extrapolated to the 100 % bound form are given next to each peak. (*right*) Part of the overlaid 2D [^{15}N, ^{1}H] HSQC spectra of the free (black) and bound (grey) ^{15}N Cyt *c*. The labels indicate the assignments of the Cyt *c* backbone amide resonances. Experiments were performed at 30^{o} C in 20 mM NaP_i 0.1 M NaCl pH 6.0.

bound form of Cyt *c* for both complexes (for details see Chapter V) – is similar for wt and T12A Cyt *c*, with only a slight increase for the latter (Figures 6.2 and 6.3). The chemical shift perturbations for both wt and T12A Cyt *c* are large (Figure 6.3), indicating that both protein complexes exist in a single orientation for most of the time (Chapter V). The majority of the residues perturbed by the interaction with CcP are the same for the two Cyt *c* variants, with the largest differences found for the groups at positions 9, 12, 13, and, to a

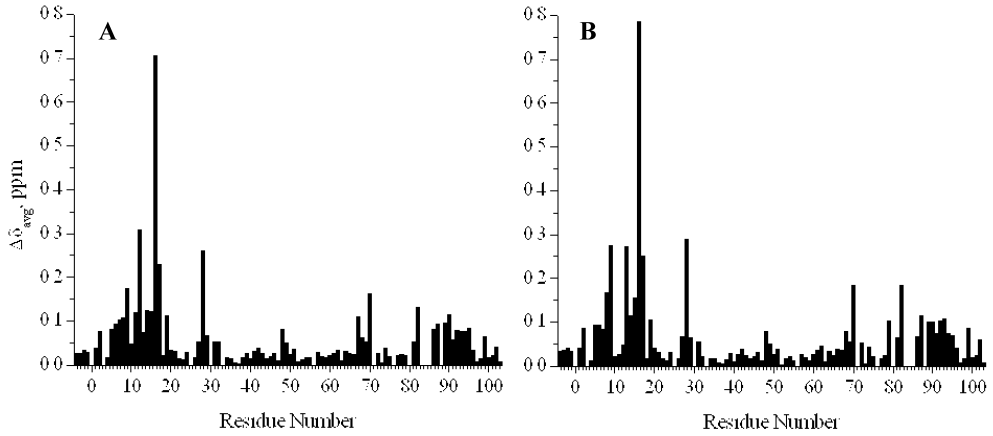

Figure 6.3. **Averaged amide chemical shift perturbations ($\Delta\delta_{avg}$) of ^{15}N Cyt *c* resonances upon binding to CcP.** The $\Delta\delta_{avg}$ for the backbone amide resonances of wt (**A**) and T12A (**B**) ^{15}N Cyt *c* in the presence of 1 molar equivalent of CcP. The $\Delta\delta_{avg}$ values are extrapolated to the 100 % bound form. The experimental conditions are given in the legend to Figure 6.2.

lesser extent 79 and 82 (Figure 6.3). It is likely that the observed differences arise from the local changes at the interface of the complex.

The NMR experiments performed at two different temperatures, 30° and 40° C, show that binding of both wt and T12A Cyt *c* leads to larger chemical shift perturbations at the lower temperature. Such enhancement of the binding shifts is most apparent in the 1D spectra of the complex (Figure 6.4). While a similar trend is observed in the 2D HSQC spectra, the difference in the size of the binding shifts at two temperatures is smaller ($\Delta\Delta\delta_{avg} < 0.05$ ppm). For the HSQC resonances, the size of the temperature-induced shifts

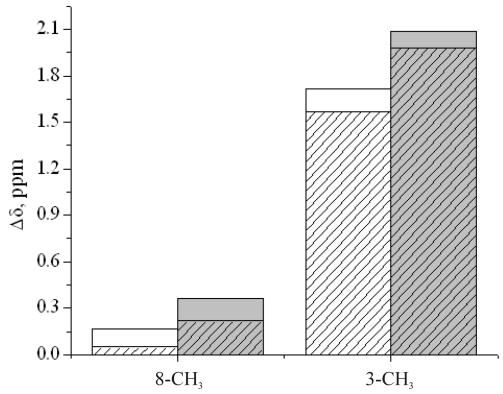

Figure 6.4. **Chemical shift perturbations of Cyt *c* resonances upon binding to CcP at different temperatures.** The binding shifts ($\Delta\delta$) of the hyperfine-shifted resonances in the 1D ^{1}H NMR spectra of wt (white) and T12A (grey) Cyt *c* in the presence of 1 molar equivalent of CcP at 30° C (clear bars) and 40° C (hatched bars). All $\Delta\delta$ are extrapolated to the 100 % bound form. The labels indicate Cyt *c* haem resonances. The experimental conditions are given in the legend to Figure 6.2.

is proportional to that of the binding perturbations (data not shown), suggesting a general, uniform effect of the temperature. For both wt and T12A Cyt *c*, the temperature-dependent differences seen in both 1D and 2D NMR spectra can be attributed to the alteration of protein dynamics within the complex or the changes in the hydration properties of the interface (see below).

Paramagnetic relaxation enhancement NMR

Solution Structure of T12A Cyt *c* – CcP Complex. We have used site-specific spin-labelling in combination with PRE NMR spectroscopy to solve the structure of T12A Cyt *c* – CcP complex in solution. Following the procedure described in Chapter III, we have converted the observed intermolecular PREs – caused by an MTSL spin-label attached to the surface of CcP and detected on the Cyt *c* backbone amides – into distance restraints (Table C1 in Appendix C), which were used in the structure calculations. Multiple rigid-body structure calculation runs have consistently produced a single cluster of solutions (data not shown), analogously to the wt complex (Figure 3.9, p. 57). Overlay of the solution structures of the T12A Cyt *c* – CcP and wt Cyt *c* – CcP complexes shows that the two structures are very similar, with 1.4 Å rmsd between the Cyt *c* molecules (Figure 6.5). Consistent with the results of the chemical shift perturbation analysis (see above), it appears that T12A mutation of Cyt *c* does not alter the structure of the dominant form of Cyt *c* – CcP complex. Similar

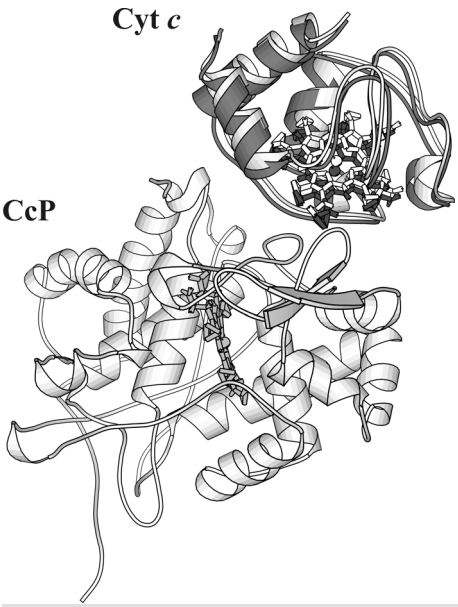

Figure 6.5. **Comparison of the solution structures of the wt Cyt *c* – CcP and T12A Cyt *c* – CcP complexes.** The CcP molecules are superimposed, and the Cyt *c* backbones in the variant and wt complexes are shown in dark and light grey, respectively. Haem groups for both proteins are in sticks. The positional backbone rmsd between the two Cyt *c* molecules is 1.37 Å. The coordinates for the solution structure of the wt complex were taken from the PDB entry 2PB8 (Chapter III).

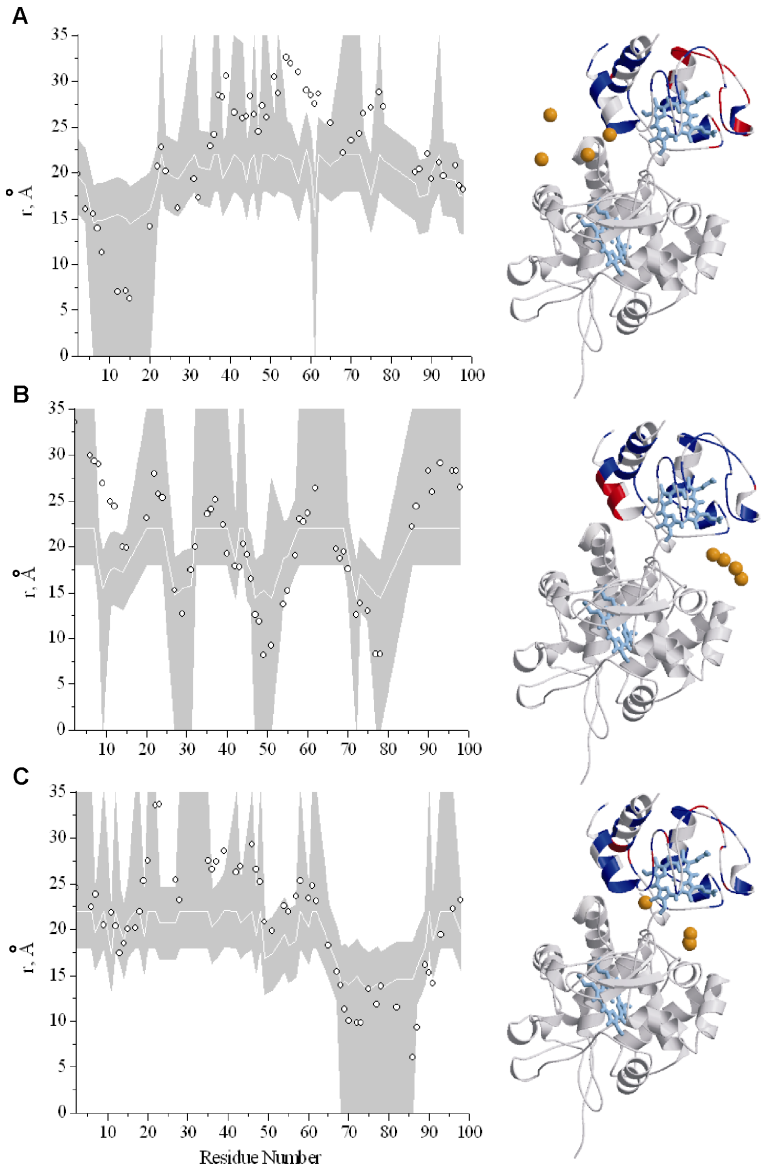

Figure 6.6. **Violation analysis of the best solution structure for the T12A Cyt *c* – CcP complex.** The graphs illustrate the distances from the Cyt *c* backbone amide protons in the lowest-energy structure (open circles) to the averaged position of the oxygen atom of MTSL attached to CcP at N38C (**A**), N200C (**B**), and T288C (**C**). The white line and the shaded area indicate the PRE-derived distances and error margins, respectively, used in the structure calculations. On the right are cartoon representations of the lowest-energy structure, indicating the residues with satisfied (blue) and violated (red) restraints. Haem groups for both proteins are in cyan. For each of the MTSL positions, four oxygen atoms that were used for ensemble averaging in the structure calculations are shown as orange spheres. For details see Materials and Methods of Chapter III.

conclusions have been drawn for R13A Cyt *c* variant (Chapter V), suggesting that point mutations at the interface of Cyt *c* – CcP complex do not influence the structure of its major form.

Dynamics in T12A Cyt *c* – CcP Complex. Some of the distance restraints are violated in the lowest-energy T12A Cyt *c* – CcP structure (Figure 6.6), implying the presence of additional protein-protein orientations within this complex (Chapter IV). Both the size and the distribution of restraint violations (Figure 6.6 and Tables C1 and C2 in the Appendix C) are similar to those observed in the wt Cyt *c* – CcP complex (Figure 4.1, p. 74). The relative amount of violated restraints – 17 % for T12A Cyt *c* and 21 % for wt Cyt *c* (Table C2 in the Appendix C) – is again similar for both complexes. Together with the findings of the chemical shift perturbation analysis (see above), these results suggest that both the fraction of time spent and the extent of the conformational space sampled by the proteins in the dynamic encounter state is the same for both Cyt *c* – CcP complexes. It appears that, while increasing the binding affinity of the complex, T12A mutation of Cyt *c* does not affect the specificity of the interaction.

Isothermal titration calorimetry

Determination of Binding Parameters at Different Temperatures. The binding of wt and T12A Cyt *c* to CcP has been investigated by ITC at four different temperatures: 293, 303, 308, and 313 K. While for T12A Cyt *c* full binding isotherms have been obtained in each case, for wt Cyt *c* complete titration curves have been constructed only at 303 and 313 K. At two other temperatures, 293 and 308 K, only the binding enthalpy (ΔH_B) has been determined by adding a small amount of wt Cyt *c* to the large excess of CcP[209]. Representative ITC curves for the binding of wt and T12A Cyt *c* are shown in Figure 6.7, and the thermodynamic parameters at different temperatures are summarized in Table 6.1. All data have been corrected for the heat of dilution of Cyt *c* that was estimated from the titration of the corresponding Cyt *c* variant into the buffer solution. Under the conditions used, the binding of wt and T12A Cyt *c* is exothermic in the experimental temperature range (Table 6.1). In all titration experiments, enough heat is released for an accurate analysis of binding isotherms (Figure 6.7). For all protein complexes investigated in this work, the titration curves – analysed with 1:1 and 2:1 binding models – fit best to a 1:1

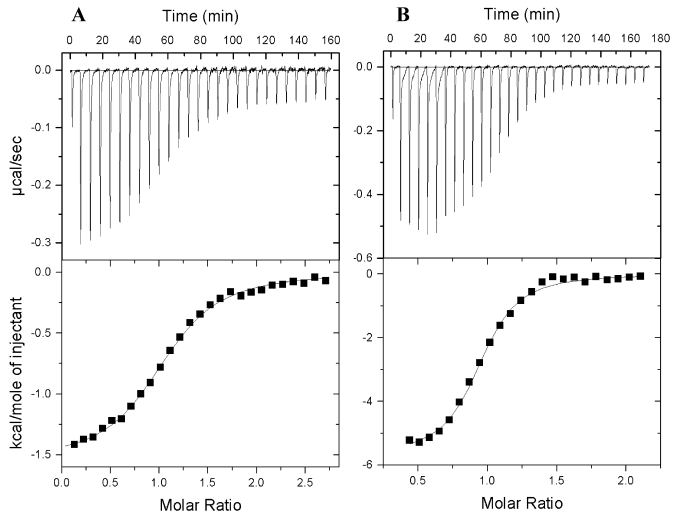

Figure 6.7. **Representative ITC binding curves.** Binding of wt (**A**) and T12A (**B**) Cyt *c* to CcP at 303 K. The top and bottom panels show, respectively, the raw data after the baseline correction and the integrated data corrected for the heat of dilution of Cyt *c*. The solid line in the bottom panel is the best fit of the data to the 1:1 binding model. The thermodynamic binding parameters and experimental conditions are given in Table 6.1.

model, suggesting that no detectable binding of the second Cyt *c* takes place under the conditions used, which is consistent with the results of our previous study (Chapter V).

Interaction of wt Cyt *c* with CcP. The thermodynamic parameters for the wt Cyt *c* – CcP complex formation obtained in this work are similar to those reported before[127,128] (Chapter V). In particular, the observed binding of wt Cyt *c* to CcP – mostly driven either by ΔS (303 K) or by ΔH (313 K) – is enhanced at higher temperature as evidenced by a slight decrease of ΔG_B (Table 6.1 and Figure 6.8), in agreement with an earlier report[127]. However, as ΔG_B for the wt complex has been determined only at two temperatures, small differences between the two values should be interpreted with care as, due to enthalpy-entropy compensation, these could represent a mere fluctuation rather than a trend.

Interaction of T12A Cyt *c* with CcP. Contrary to our expectations, T12A mutation of Cyt *c* stabilizes complex formation with CcP. At 303 and 313 K ΔG_B is decreased by 12 % and 19 %, respectively, relative to that of the wt (Figure 6.8), with the corresponding 4 – 10-fold increase in the binding constant (Table 6.1). At both temperatures, ΔS_B for the binding of T12A Cyt *c* is decreased relative to that for the wt, so that the gain in the binding energy arises solely from a favourable enthalpy term, which is

Table 6.1. **Thermodynamic parameters of Cyt *c* – CcP binding obtained from ITC experiments[a]**

Cyt *c*	T, K	N[b]	K_B[c]	ΔG_B	ΔH_B[d]	$-T\Delta S_B$
wt	293 (2)[e]	n.d.[f]	n.d.	n.d.	-0.8 ± 0.1	n.d.
	303 (3)	1.06 ± 0.01	1.8 ± 0.2	-7.3 ± 0.1	-1.7 ± 0.1	-5.6 ± 0.2
	308 (2)[e]	n.d.	n.d.	n.d.	-2.8 ± 0.3	n.d
	313 (2)	1.07 ± 0.01	2.3 ± 0.2	-7.7 ± 0.1	-5.7 ± 0.2	-2.0 ± 0.1
T12A	293 (1)	0.93 ± 0.01	26 ± 5	-8.6 ± 0.1	-4.0 ± 0.1	-4.6 ± 0.2
	303 (3)	0.97 ± 0.06	17 ± 2	-8.7 ± 0.1	-5.5 ± 0.3	-3.2 ± 0.3
	308 (1)	1.14 ± 0.02	14 ± 5	-8.2 ± 0.1	-6.9 ± 0.1	-1.3 ± 0.3
	313 (2)	1.04 ± 0.01	9.8 ± 0.1	-8.6 ± 0.1	-10.6 ± 0.2	2.0 ± 0.1

[a] Experiments were performed in 20 mM NaP_i 0.1 M NaCl pH 6.0. The units of ΔG_B, ΔH_B, and $-T\Delta S_B$ are kcal·mol^{-1}. Number of experiments performed at each temperature is given in parentheses. For the repeated experiments, the errors are the standard deviations from the mean. For the experiments performed only once, the uncertainties are the errors of the fit of the integrated data. [b] Stoichiometry of binding. [c] Equilibrium binding constant, 10^5 M^{-1}. [d] The ΔH_B values corrected for the heat of buffer ionisation are 0.42 kcal·mol^{-1} more positive than those shown (Chapter V). [e] A full binding isotherm has not been obtained in these experiments. [f] The parameter has not been determined.

increased 2 – 3-fold with respect to that of the wt (Figure 6.8). The increase in ΔH_B suggests that additional intermolecular interactions, absent from the wt complex, may stabilize the T12A Cyt *c* – CcP association.

The thermodynamic parameters for binding of T12A Cyt *c* at four different temperatures are plotted in Figure 6.9. While ΔH_B is large and negative in the experimental range of temperatures, the entropy term, $-T\Delta S_B$, varies from negative to positive and changes sign between 308 and 313 K. At lower temperatures both ΔH_B and ΔS_B promote the binding, while at higher temperatures the binding is clearly enthalpy-driven.

Effect of Temperature on the Binding Energy. In contrast to wt Cyt *c* – CcP complex formation, which was reported to be enhanced with increasing temperature[127], there is no correlation between the changes in ΔG_B and the temperature for T12A Cyt *c* –

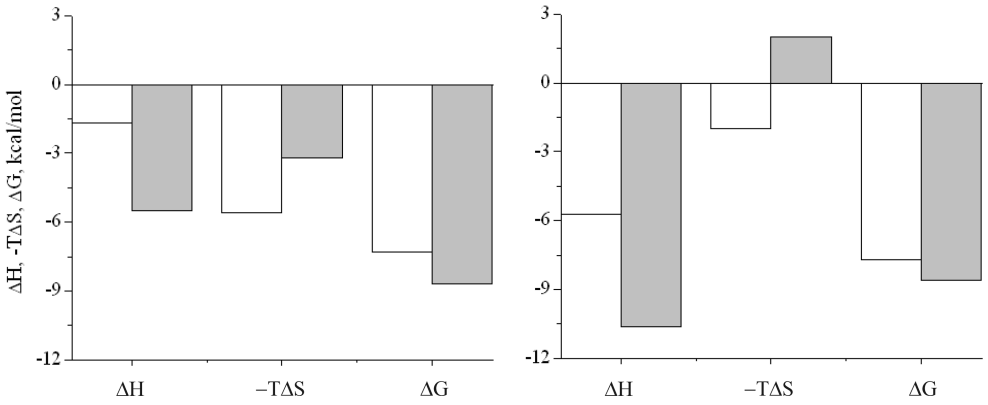

Figure 6.8. **Thermodynamic parameters for the Cyt *c* – CcP complex formation.** ΔH, -TΔS, and ΔG for the binding of wt (white) and T12A (grey) Cyt *c* to CcP at 303 K (left) and 313 K (right). The histograms are based on the Table 6.1.

CcP (Figures 6.9 and 6.10 A, and Table 6.2). The observed temperature-independence of the binding constant is due to enthalpy-entropy compensation, a familiar feature of protein-protein interactions[215].

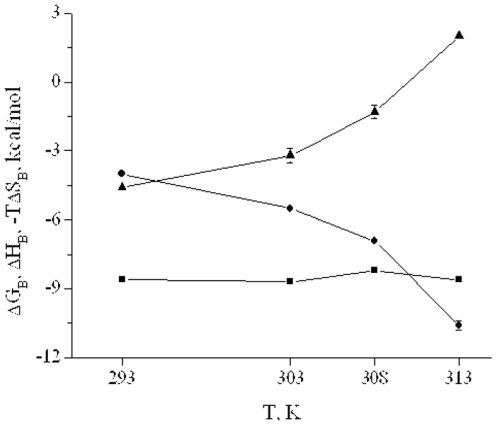

Figure 6.9. **Effect of temperature on T12A Cyt *c* – CcP binding parameters.** ΔG_B, ΔH_B, and $-T\Delta S_B$ are indicated by squares, circles, and triangles, respectively. For the data points without error bars, the error is less than the size of the symbol. This figure is based on Table 6.1.

Effect of Temperature on the Binding Constant: van't Hoff Enthalpy. Unlike ΔG_B, the binding constant of T12A Cyt *c* – CcP complex scales linearly with the temperature (Figure 6.10 B). It is clear that T12A Cyt *c* and CcP bind tighter at lower temperature (Figure 6.10 B and Table 6.1), which is in stark contrast to the behaviour of the wt complex[127]. We can estimate the van't Hoff enthalpy of binding (ΔH_{vH}) from the slope of the linear fit in Figure 6.10 B. While for the wt complex ΔH_{vH} is markedly different from calorimetric ΔH_B[127], for T12A Cyt *c* – CcP

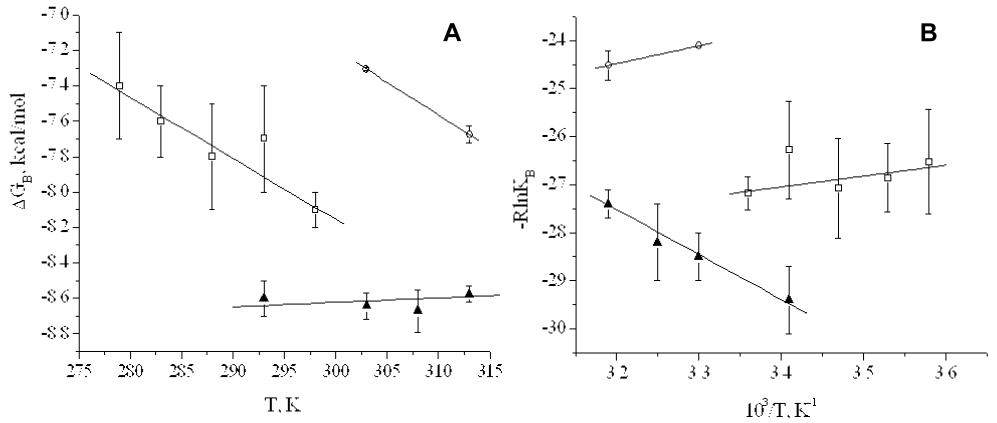

Figure 6.10. **Effect of temperature on the binding of wt and T12A Cyt *c* to CcP.** ΔG_B (**A**) and $-RlnK_B$ (**B**) for the binding of the wt Cyt *c* (open circles), T12A Cyt *c* (filled triangles), and wt Cyt *c* from ref. 127 (open squares) at different temperatures. The solid lines represent linear (**A**) or weighted linear (**B**) fits of the data, with the slopes given in the Table 6.2.

interaction ΔH_{vH} = -9.4 ± 0.7 kcal·mol^{-1} (Table 6.2) is in agreement with the experimental ΔH_B values (Table 6.1).

It was shown that for many biomolecular interactions ΔH_{vH} and ΔH_B do not match[227]. This discrepancy was attributed to a widely-accepted, yet erroneous derivation of the simplified van't Hoff equation that is used to deduce ΔH_{vH}[228,229]. It appears that ΔH_{vH} and ΔH_B are expected to be the same only if the binding reaction follows a simple two-state transition between free and bound molecules[227,230] or if the observable used to infer ΔH_{vH}

Table 6.2. **Thermodynamic parameters extracted from the temperature-dependence of ΔG_B, ΔH_B, and K_B.**

Cyt *c*	$\delta(\Delta G_B)/\delta T$[a]	ΔH_{vH} [b]	ΔC_p
wt (ref.127)	-35 ± 5	2.3 ± 1.6	-216 ± 62[c]
wt	-37	3.7	-85 to -596[d]
T12A	3 ± 2	-9.4 ± 0.7	-147 to -734[d]

The slopes of the linear fits of the data in: [a] Figure 6.10 A, [b] Figure 6.10 B, and [c] Figure 6.11. [d] The values are estimated from the first two and the last two data points of the respective curves in Figure 6.11. The units of $\delta(\Delta G_B)/\delta T$ and ΔC_p are cal·mol^{-1}K^{-1}, and that of ΔH_{vH} is kcal·mol^{-1}. The uncertainties are the errors of the fits.

reflects all phenomena associated with protein binding (*e.g.* solvent reorganisation, buffer ionisation, conformational change, *etc.*)[207]. With these considerations in mind, the large discrepancy between ΔH_{vH} and ΔH_B for wt Cyt *c* – CcP complex was interpreted as an evidence for binding-induced solvent re-arrangement[127]. As for T12A Cyt *c* – CcP the two enthalpies are nearly equal, we propose that the net solvent re-organisation is less profound in the variant than in the wt complex (see below) and, therefore, the T12A Cyt *c* – CcP interaction is closer to a simple two-state binding model.

Effect of Temperature on the Binding Enthalpy: Heat Capacity Change. The constant-pressure heat capacity change (ΔC_p) – yet another fundamental thermodynamic parameter of a chemical reaction in addition to ΔG, ΔH, and ΔS – can be estimated from the local slope of the linear trend in the plot of ΔH_B versus temperature[207]. For both wt and T12A Cyt *c*, ΔH_B decreases with increasing temperature (Figure 6.11), in agreement with a previous study of the wt complex[127].

However, the decrease is not linear, implying temperature-dependence of ΔC_p. Analysis of the earlier data for the wt complex[127] – included for comparison in Figure 6.11 – shows a similar deviation from linearity, not commented upon by the authors. Admittedly, the data of Wang & Pielak[127] resist unequivocal interpretation, as a single data point, at 293 K, is responsible for most of the deviation (Figure 6.11). It can be argued that if this point is omitted, the linearity is restored; however, taken at the face value, the data fit poorly to the linear trend (Figure 6.11 and Table 6.2). The shape of the ΔH_B temperature-dependence curves (Figure 6.11) and the range of ΔC_p values (Table 6.2) – estimated from the first two and the last two data points of the curves in Figure 6.11 – are the same for the binding of T12A and wt Cyt *c*.

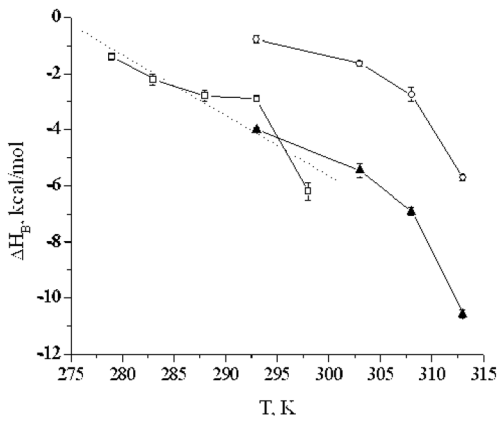

Figure 6.11. **Effect of temperature on the binding enthalpy of the Cyt *c* – CcP complexes.** The data for the binding of wt Cyt *c* (open circles), T12A Cyt *c* (filled triangles), and wt Cyt *c* from ref. 127 (open squares). The broken line represents the linear fit of the reported data[127] (see Table 6.2).

In the literature, the temperature-dependence of ΔC_p has been attributed either to large binding-induced conformational rearrangements[231] or to pre-existent, temperature-dependent conformational equilibria[232]. As seen in the crystal structure of the complex[107] and confirmed by solution NMR studies[129] (Chapter III), the only conformational change induced by the binding of Cyt *c* to CcP is re-organisation of Cyt *c* Q16 side-chain, which does not constitute a large rearrangement. Furthermore, both Cyt *c*[34] and CcP[87] exist in a single isomer form; therefore, possible conformational equilibria in solutions of individual proteins can be ruled out. As for the Cyt *c* – CcP complex the two suggested contributions to the temperature-dependence of ΔC_p are unlikely, the observed deviation from the linearity in ΔH_B plots versus temperature is difficult to rationalize. One explanation could be provided by a hypothesis – yet to be tested experimentally – that the binding-induced solvent rearrangement varies at different temperatures thereby, giving rise to the observed deviation (see below).

Comparison of the Calculated and Experimental Thermodynamic Parameters. A number of semi-empirical methods allow to estimate ΔH_B and ΔC_p from the change of the buried surface area accompanying a biomolecular association (see ref. 207 and references therein). For the complex of Cyt *c* and CcP, these have been calculated before[127] and, together with the thermodynamic parameters determined experimentally in this work, are collected in Table 6.3. In the following discussion, we assume that the thermodynamic parameters predicted for the binding of wt Cyt *c* are also valid for T12A variant, which is expected given the similarity of the solution structures for the wt Cyt *c* – CcP and T12A Cyt *c* – CcP complexes.

Table 6.3. **Estimated and experimental thermodynamic parameters for Cyt *c* – CcP[a].**

	ΔH_B	ΔC_p
wt	-0.8 to -5.7	-85 to -596
T12A	-4.0 to -10.6	-147 to -734
Theoretical values	-6.5 to -11.3[233] -10.0 to -10.9[234]	-133 to -180[233] -162 to -187[235]

[a] The experimental values, taken from Tables 6.1 and 6.2. The estimated values have been calculated by Wang & Pielak[127] using the methods referenced by the superscript next to each value. The units of ΔH_B and ΔC_p are kcal·mol^{-1} and cal·mol^{-1}K^{-1}, respectively.

Although no accurate comparison can be made between the calculated and the observed, temperature-dependent ΔC_P values, these seem to be in reasonable agreement for both wt and T12A Cyt *c* (Table 6.3). In contrast, the correlation between the calculated and the observed values of ΔH_B is different for the two complexes. For the wt Cyt *c* – CcP complex, the estimated ΔH_B values are more exothermic than those determined experimentally (Table 6.3), in agreement with a previous report[127]. On the contrary, for the binding of T12A Cyt *c*, there is a good correspondence between the estimated and experimentally determined ΔH_B values (Table 6.3), with a stronger correlation at higher temperatures (see Table 6.1). Such agreement suggests that the assumptions used to develop the models are valid for the binding of T12A, but not wt, Cyt *c*. While most of the approximations inherent in these models – such as the absence of large conformational changes or complexes of varying stoichiometry – are reasonable for both protein complexes, the assumption that no large water rearrangement takes place upon binding is controversial. As discussed in the section below, different hydration properties of the two interfaces could explain most of the differences observed in the binding of wt and T12A Cyt *c* to CcP.

Possible role of water structuring in the binding of Cyt c to CcP

The combination of the observed $\Delta C_p < 0$ and $\Delta S_B > 0$ indicates that the binding of both wt and T12A Cyt *c* is accompanied by the solvent release associated with the hydrophobic effect[236]. As discussed above, solvent reorganization in the wt Cyt *c* – CcP complex could explain the discrepancies between the experimental values of ΔH_{vH} and ΔH_B, as well as between the predicted and the observed ΔH_B and ΔC_p values[127]. As the match between both sets of parameters is much better for the binding of T12A Cyt *c*, it can be suggested that water release from the interface of T12A Cyt *c* – CcP complex is either attenuated or counterbalanced by the binding-induced structuring of water molecules. However, the former is unlikely as, given similarity of the solution structures for the wt Cyt *c* – CcP and T12A Cyt *c* – CcP, the buried surface area is expected to be similar in both complexes. Therefore, we propose that the binding of T12A Cyt *c* to CcP is accompanied by organisation of water molecules at the interface.

In addition to the matching predicted and observed parameters, structuring of water can further explain the mutation-induced changes in ΔS_B and ΔH_B. As was shown by ITC and crystallographic study of an antigen-antibody association[237], ordering of water molecules at the protein interface reduces ΔS_B and enhances ΔH_B. This is exactly what we observe comparing the binding of wt and T12A Cyt *c*. As discussed in Chapter V, there is a crystallographic evidence for the structured water molecules at the interface of wt Cyt *c* – CcP complex[118]. If such water organisation occurs in the solution complex, our experimental results would suggest that T12A mutation promotes it even further. In this case the local structural changes attendant upon water rearrangement would explain the large chemical shift perturbations of L9 and R13 residues of T12A Cyt *c* that are not affected in the complex of wt Cyt *c* (Figure 6.3).

Our results indicate a likely variation of solvent activity at different temperatures in Cyt *c* – CcP complex, which could give rise to the observed temperature-dependence of ΔC_p. If water release from the interface is promoted at lower temperatures or, more likely, structuring of water is enhanced at higher temperatures, this would explain the observed decrease in ΔS_B and increase in ΔH_B with the rising temperature. Interestingly, similar temperature-dependence of ΔS_B and ΔH_B has been observed for another protein-protein interaction mediated by bound water[237]. Moreover, temperature-promoted water structuring could explain why for T12A Cyt *c* – CcP complex the estimated ΔH_{vH} and the predicted ΔH_B agree better with the experimental ΔH_B values at higher temperature, indicating a net balance between water uptake and release. Finally, the increased chemical shift perturbations at lower temperature could be caused by an augmented desolvation of the interface, which, together with the protein dynamics, is thought to determine the size of the binding sifts in the transient protein complexes (Chapter V).

Concluding remarks

Our results suggest that T12A mutation of Cyt *c* increases the affinity of Cyt *c* – CcP complex without affecting the specificity of the interaction. We argue that the affinity increase is likely mediated by ordering of water molecules at the interface. Though this hypothesis has yet to be experimentally tested, it would explain most of the differences in

the binding behaviour of wt and T12A Cyt *c*. Moreover, a suggested differential solvent activity at various temperatures could account for the observed temperature-dependence of the thermodynamic parameters for Cyt *c* – CcP interaction.

Materials and Methods

Cyt *c* T12A mutation has been introduced by site-directed mutagenesis using the Quik Change™ polymerase chain reaction protocol (Stratagene, La Jolla, CA) with the plasmid pUCcc as a template (for details see Appendix D), and the construct has been verified by DNA sequencing. Both unlabelled and ^{15}N isotopically-enriched T12A Cyt *c* has been expressed and purified analogously to the wt protein (Chapter II and Appendix B). The isolation of wt CcP and its single-cysteine variants used in the PRE analysis of the complex is reported in Chapter III, and the detailed protocol can be found in the Appendix B at the back of this thesis. The ITC and NMR sample preparations and experiments are described in detail in Chapter V. The PRE NMR analysis and the structure calculation of the T12A Cyt *c* – CcP complex have been carried out following the procedures used for the wt complex (Chapter III).